MRiLab: Fast Realistic MRI Simulations Based on Generalized Exchange Tissue Model

Fang Liu[1], Walter F. Block [2], Richard Kijowski [1] and Alexey Samsonov[1].

[1]Departments of Radiology, and [2]Biomedical Engineering, University of Wisconsin, Madison, WI, USA

Introduction: Numerical simulations greatly facilitate understanding and development of MRI methods. The complexity of simulations needed for accurate description of modern MRI systems calls for development of dedicated software solutions. One highly desired feature largely missing in the existing MRI simulators is ability to simulate a response from multi-pool spin models of an arbitrary configuration. Such feature would allow accommodating a wide variety of simulation tasks including the characterization of multiple tissue compartments, partial voluming modeling, and quantification of perfusion/permeability. Previously, we have developed an open-source, extensible simulation software MRiLab (http://sourceforge.net/projects/mrilab) which leverages the power of modern Graphical Processing Units (GPU) for fast realistic 3D simulations [1]. The modularized simulation workflow combined with flexible function tools enable simulations suitable for multiple research purposes including investigating new RF pulses, sequence design, parallel coil transmitting and receiving, B0 and B1 field analysis, 4D dynamic MRI. Here, we present the next generation of the software that enhances MRiLab pipeline with ability to use arbitrary multi-compartmental models to further facilitate realistic MRI simulations.

Methods: *Generalized Multi-Pool Tissue Model:* The generalized exchange model implemented in MRiLab consists of N_F free proton pools all inter-connected by the magnetization exchange (MT) pathways, and N_B bound proton pools exchanging with the free pools (Fig. 1). Attributes of each pool include relative proton fraction, relaxation parameters, and chemical shift spectra. The free proton pools are reserved to model compartments with measurable transverse magnetization (e.g., water, fat, solute proton exchange compounds), and the bound proton pools to model semi-solid tissue macromolecular content non-visible on standard MRI (e.g., myelin, muscle fibers, collagen). *Software Implementation:* Responses of free and bound proton pools are simulated using the finite differential Bloch-McConnell equations in the rotating frame [2] and MT saturation formalism [3], respectively. The simulation core code for calculating the mathematical equation is implemented in C language for high simulation performance. Compute Unified Device Architecture (CUDA) and Open Multi-Processing (OpenMP) were used for GPU and multi-core CPU parallel simulation computation. A highly interactive user interface is developed using Matlab GUI Development Environment. The current version of MRiLab is composed of a main simulation panel, accessory function panels, discrete Bloch-equation solving kernel, image reconstruction and analysis toolkit. *Evaluation:* Two tissue models were used to evaluate MRiLab: The first model describes glycosaminoglycan CEST (gagCEST) effect [4] and consists of several pools representing macromolecules, water, and chemically shifted (δ=+1.0ppm) OH- hydroxyl groups (Fig. 2a). The second model is used to study MT imaging with gradient echo (GRE) sequences in the presence of fat (Fig. 3a). According to the recent findings on nonexistence of efficient mechanisms of MT from fat to either of the proton pools [5], no exchange pathways were set for fat. Agar (2%)+fat (0%, 30%, 50%)+water phantoms were created and imaged at 3T using multi-echo MT GRE both with and without MT pulse. Artificial images corresponding to the given phantom layout, MRI system, and pulse sequence configuration were simulated in MRiLab using literature T1/T2 values for agar and fat, and multi-peak chemical shift fat model. Both acquired and simulated images were supplied to calculate MT ratio (MTR) for all acquired echoes.

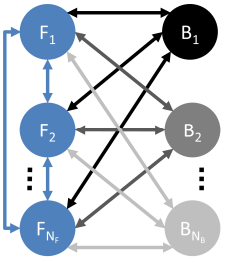

Figure 1. *Generalized MRiLab tissue model.*

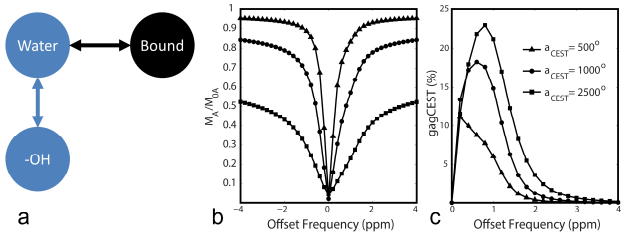

Figure 2. a: *Configuration of MRiLab model to simulate gagCEST;* ***b,c:*** *gagCEST Z-Spectrum and asymmetry plots, respectively, simulated at different CEST saturation flip angles.*

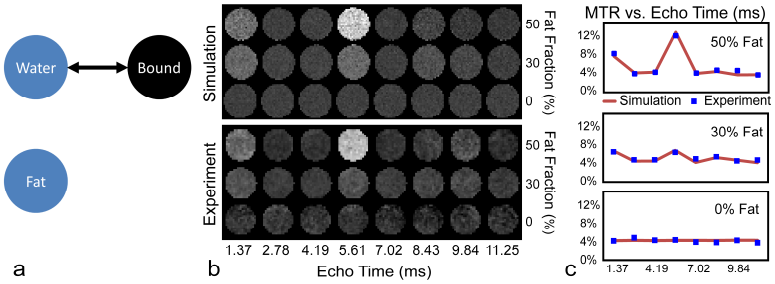

Figure 3. a: *Configuration of MRiLab model to simulate MTI in the presense of fat.* ***b:*** *Simulated (top) and measured (bottom) MTR maps,* ***c:*** *Corresponding ROI-averaged plots. Note visual similarity of simulated and experimental MTRs and ROI-averaged plots and variability of MTR with fat fraction and echo time.*

Results: Figure 2b,c shows MRiLab-simulated gagCEST Z-Spectra and gagCEST asymmetry plots, which agree well with those published in literature [4]. The asymmetry plot (Fig. 2b) demonstrates an increase of gagCEST effect at around 1.0ppm reflecting the presence of hydroxyl protons. Figures 3b,c shows simulated and measured MTRs from agar+fat+water phantoms. Note stable MTR behavior for a fat-free phantom. Despite the same macromolecular fraction for all phantoms, there is a strong echo-time dependence of MTR in fatty phantoms due to complex interaction of water and fat components (Fig. 3b). The experimental observations are excellently predicted by MRiLab simulations (Fig. 3c).

Discussion: This abstract demonstrates the feasibility using MRiLab for simulation of MRI of tissues represented by an arbitrary multi-pool models. We found that GPU parallel computing model can effectively handle the computational complexity associated with the incorporation of such models into MRI simulation pipeline. The new feature may be important to improve understanding of signal behavior in standard MRI approaches and to facilitate development of modern MRI approaches targeting characterization of biologically important tissue microstructural features and microenvironment.

REFERENCES: [1] Liu F, et al. ISMRM 2014, 5244. [2] McConnel HM, JCP 1958,28:430. [3] Henkelman RM, et al, MRM 1993;29(6):759. [4] Ling W, et al. PNAS 2008;105:2266. [5] Chen JH, et al. MRM 2006;55:1246.

ACKNOWLEDGEMENTS: The work was supported by NIH (R01NS065034).